Optics and Lasers in Engineering 150 (2022) 106849

Contents lists available at ScienceDirect

Optics and Lasers in Engineering

journal homepage: www.elsevier.com/locate/optlaseng

Design and fabrication of monolithically integrated metalens for higher effective fill factor in long-wave infrared detectors

Huwang Hou [b], Yiyuan Zhang [a], Zhendong Luo [a], Peng Zhang [a,*], Yang Zhao [a,c,*]

[a] CAS Key Laboratory of Mechanical Behavior and Design of Materials, Department of Precision Machinery & Precision Instrumentation, University of Science and Technology of China, Hefei 230022, China

[b] CAS Key Laboratory of Mechanical Behavior and Design of Materials, Department of Modern Mechanics, University of Science and Technology of China, Hefei 230022, China

[c] Key Laboratory of Precision Scientific Instrumentation of Anhui Higher Education Institutes, University of Science and Technology of China, Hefei 230022, China

ARTICLE INFO

Keywords:
Metalens
Infrared detector
Fill factor
Integration
Focal plane array (FPA)

ABSTRACT

Infrared imaging technology has been a worldwide research focus with various significant applications in the military and surveillance fields. Due to the complicated structure of the infrared imaging element, the photosensitive area only occupies quite a small part of each element, resulting in a low fill factor and thus limited utilization efficiency of incident light. By integrating a polarization-independent, wide-band focusing metalens into the imaging element of the long-wave infrared detector, the effective fill factor can be significantly improved. The monochromatic focusing efficiency of the metalens is up to 86%, and the average focusing efficiency in the wide spectral from 8 μm to 14 μm reaches 80%. The focusing measurement results demonstrate that the fabricated metalens can be used as a light concentrator to improve the detection sensitivity. The micro-optical metalens is flat and ultra-thin shaped, which is composed of sub-wavelength silicon pillars. Due to its compatibility with the detector manufacturing process, the metalens can be scaled up for a large micro-metalens array monolithically integrated with an infrared focal plane array(FPA).

1. Introduction

Infrared imaging is widely used in military reconnaissance, medical diagnosis, security inspection, vehicle night vision, and other fields [1] with a tendency to develop higher spatial resolution and detection sensitivity. Researchers improved the performance of detectors by finding substitute materials [2,3], proposing new structures[4,5], and exploring new signal readout methods [6]. Moreover, the performance of detectors can also be enhanced by improving the fill factor, which is defined as the ratio of the photosensitive area to the whole pixel area. In order to suppress the dark current of photon detectors, the photosensitive area of the detector is often much smaller than its pixel area because the dark current is proportional to the photosensitive area [7], which results in a low fill factor for incident infrared light. Similarly, an insulating leg is required for thermal detectors to reduce the heat loss [2], and therefore the fill factor is limited. Therefore, spherical microlenses [8,9] formed by heat reflow and diffractive microlenses [10,11] were used to converge the incident light, thereby increasing the effective fill factor. Nevertheless, the curved surface of the spherical lens is hard to fabricate, and the accuracy is difficult to guarantee. To achieve higher efficiency, the diffraction lens needs to be fabricated into a multi-height levels grating structure, which is complicated to process. In recent years, metasurface composed of subwavelength structures has been extensively studied [12–14]. Metasurface lenses, polarizers, zone plates, holograms, and other metasurfaces have been applied to various devices [15–17]. Because the metalens is composed of planar unit structures, the fabrication process is of compatibility with the general MEMS technique and capability to scale up. The refractive microlens and diffractive microlens are expected to be replaced by the metalens. Solid-immersion metalens for mid-wave infrared (MWIR) FPA was proposed by Zhang, S. et al., with a focusing efficiency of 52% [18]. The simulation method was used to design a metalens integrated with TeCdHg MWIR photodetector and verify its dispersion tolerance and angular response [7]. Long-wave infrared (LWIR) imaging is of more significance in practical applications because the peak infrared radiation spectrum of objects at room temperature is 8 to 14 μm. Some LWIR metasurfaces have been studied, such as a large numerical aperture imaging lens [19]. However, the investigation of broad-band metalenses integrated with LWIR detectors is very limited.

In this work, we propose the design and fabrication of polarization-insensitive and wide-band LWIR metalenses for LWIR FPA. Fig. 1 demonstrates the monolithic integration of a metalens and an optical readout uncooled infrared detector. The metalens concentrates the inci-

* Corresponding authors.
E-mail addresses: zhp9036@mail.ustc.edu.cn (P. Zhang), yangz1@ustc.edu.cn (Y. Zhao).

https://doi.org/10.1016/j.optlaseng.2021.106849
Received 3 August 2021; Received in revised form 20 September 2021; Accepted 11 October 2021

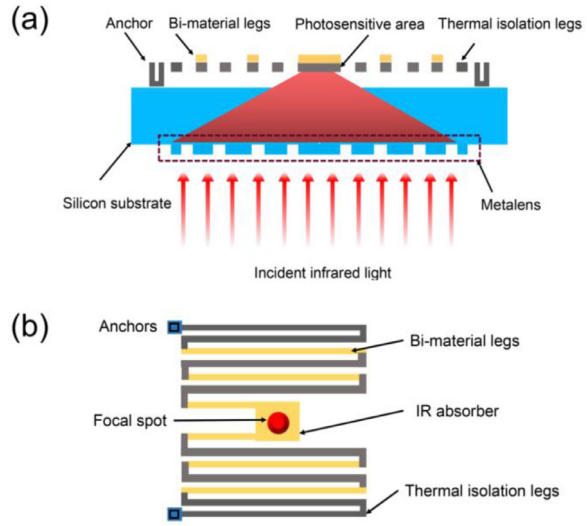

Fig. 1. (a) Illustration of the metalens integrated with the IR detector. (b) Bi-material LWIR detector.

dent infrared light into a thinner beam, enabling a small absorption plate to absorb most of the incident light and avoiding energy leakage loss. The designed metalens is composed of silicon dielectric micro-pillars. A 60 μm diameter metalens with a focal length of 300 μm is simulated with a focusing efficiency of 80% for 8~14 μm wavelength range. The measurement results show an excellent focusing effect of the fabricated metalens. The metalens can be integrated with long-wave infrared detector arrays on a large scale and is of great potential to improve the performance of infrared imaging focal plane arrays.

2. Design and simulation

2.1. Design criteria

The essence of the metalenses that can achieve beam focusing is a discrete and planar phase modulator, which includes the resonance phase, geometric phase, and propagation phase. To increase the effective fill factor of incident infrared signal on the imaging elements, the design criteria of metalens requires high transmittance, polarization-independence, broad-spectrum, high focusing efficiency, and compatibility with the manufacturing process of the FPAs. The metalens based on the metallic plasmonic antenna is not applicable due to its high ohmic loss [20]. Although the metalens based on the geometric phase [21] is independent of the incident wavelength, the total energy efficiency will not be higher than 50% because of the selectivity to the left/right-handed circularly polarization states of the incident light, which is even lower than the efficiency of some IR detectors without integrated microlenses.

A micro-metalens is designed based on silicon substrate, since silicon is a transparent material in the long-wave infrared spectrum with low absorption loss. The metalens is composed of all-dielectric (silicon) circle pillars with variable diameters. Because the phase modulation unit cell is a cylinder and of quadruple symmetry, the focusing efficiency is independent of the polarization state of the incident light. The focal spot of the lens is the Fraunhofer diffraction of the aperture at the focal plane, which is known as the Airy spot. The radius of the Airy spot is

$$R = 1.22\lambda f/nD, \tag{1}$$

where λ is the wavelength in the free space, f the focal length, n the refractive index of the medium, and D is the diameter of the lens. Since the diameter of the metalens is the same as the specific pixel size, the focal length, which equals the thickness of the substrate material, should be as small as possible to achieve a more concentrated focus of the beam. But thinner substrate requires additional wafer grinding and can make the device fragile. As long as the size of the focal spot is close to the photosensitive area, most of the energy can be absorbed by the detector. It is suitable to use a silicon wafer commonly used in processing with a thickness of 300 μm. The refractive index of silicon can be considered constant in the long-wavelength infrared spectrum, and the dispersion characteristic of the metalens is determined by the structural dispersion. According to the effective medium theory, the zeroth-order approximation of the effective refractive index requires the period of the sub-wavelength structure to be much smaller than the wavelength (approximately $\lambda/10$), which brings challenges to the fabrication process due to the ultrahigh aspect ratio of the structure [22]. Therefore, a period equaling the wavelength in the medium is adopted, and other orders term of chromatic dispersion has little effect on the focusing efficiency as shown in the following simulation. Meanwhile, the manufacturing of the structure becomes easier to achieve.

2.2. Inverse design of the metalens

With the expectation of integrating metalens into the uncooled infrared detector based on a silicon substrate with the pixel area of 60 μm x 60 μm, the diameter of the metalens is set to be 60 μm, and the focal length is equal to the thickness of the substrate, which is 300 μm. The phase modulation function of the metalens can be written as:

$$\emptyset(x, y) = 2\pi n\left(f - \sqrt{x^2 + y^2 + f^2}\right)/\lambda \tag{2}$$

where $\emptyset(x,y)$ denotes the phase at position (x,y).

Unlike general spherical lenses, a metalens converts the incident plane wave into a focused spherical wave by the sub-wavelength unit cells with the same height. Due to the complexity of the boundary conditions, it is difficult to theoretically obtain the relationship between the effective refractive index of the unit-cell and the geometric parameters. Using the software FDTD solutions based on electromagnetic wave finite-difference time-domain method, the entire metalens structure is obtained inversely through the method of parameter sweep.

The unit cell used for controlling the local phase of the metalens is a subwavelength pillar as shown in Fig. 2(a), whose period equals the wavelength in Si medium (3 μm), and the wavelength in free space here is 10 μm. The effective refractive index is close to that of air and silicon when the pillar diameter approaches 0 and the unit-cell period, respectively, which determines the maximum phase adjustment range. The phase modulation range $\Delta\emptyset$ can be written as:

$$\Delta\emptyset = 2\pi\left(n_{eff,max} - n_{eff,min}\right)h/\lambda \tag{3}$$

where, $n_{eff,max}$ and $n_{eff,min}$ are the maximum and minimum effective refractive index of the unit-cells, respectively, and h is the height of the unit cells. To cover the phase range of 2π, the height of the pillar is at least 5 μm. To avoid structures with an excessive aspect ratio, the diameter of the unit cells varies from 0.5 μm to 2.5 μm. The phase modulation map of pillars with different diameters and heights is obtained by the parameter sweep method, as shown in Fig. 2(b). It can be seen from Fig. 2(d) that the higher the pillar, the wider phase adjustment range will be achieved. However, it will bring challenges to the manufacturing process when the height is excessive. Hence, the height of 8 μm is chosen here, and its phase adjustment can cover the range of 2π. The target phase of Eq. (2) can be achieved by arranging the pillar at the position (x,y) with a diameter whose phase modulation is exactly $\emptyset(x, y)$ according to the phase modulation map. The entire metalens structure is shown in Fig. 2(f). The lens is composed of pillars of the same height. The central pillar is thick with a high duty ratio, thus a high effective refractive index and a large propagation phase can be achieved. Conversely, the pillars near the edge of the lens are thin with a low duty ratio and thus led to a low effective refractive index and a small propagation phase. By arranging the pillars carefully, the spherical phase distribution can be realized.

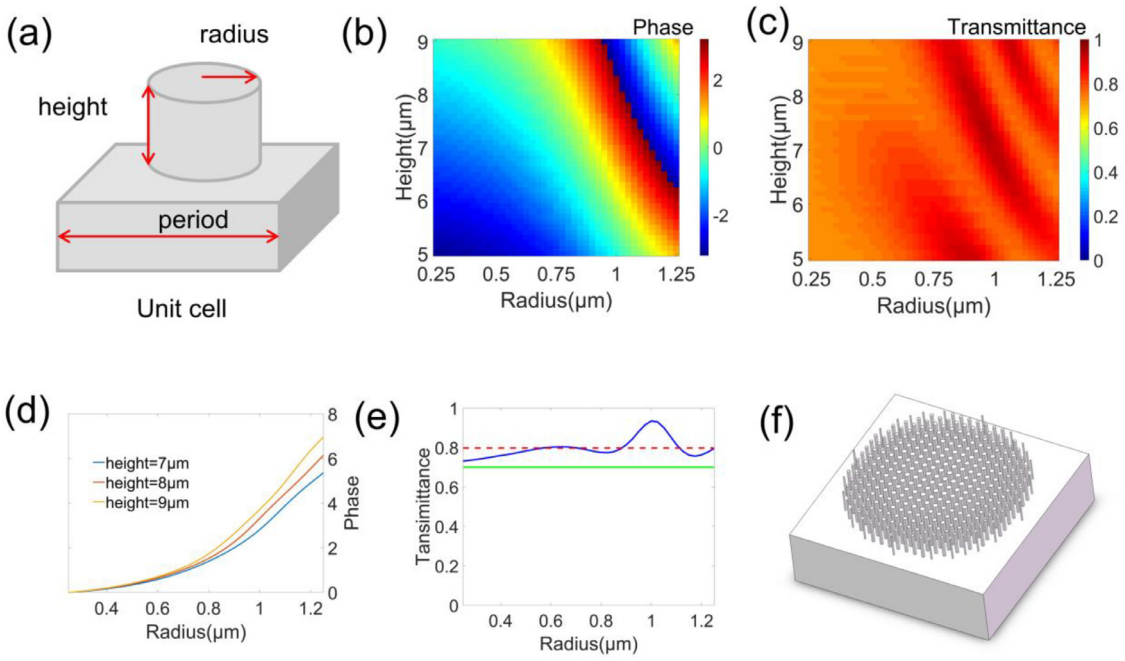

Fig. 2. Inverse design of metalens structure. (a) The unit-cell structure with 3 μm period. (b) The phase modulation map. (c) The transmittance map. (d) The phase modulation of the unit cells at different heights. (e) The transmittance of the unit-cells at the height of 8 μm. (f) Structure of the entire metalens.

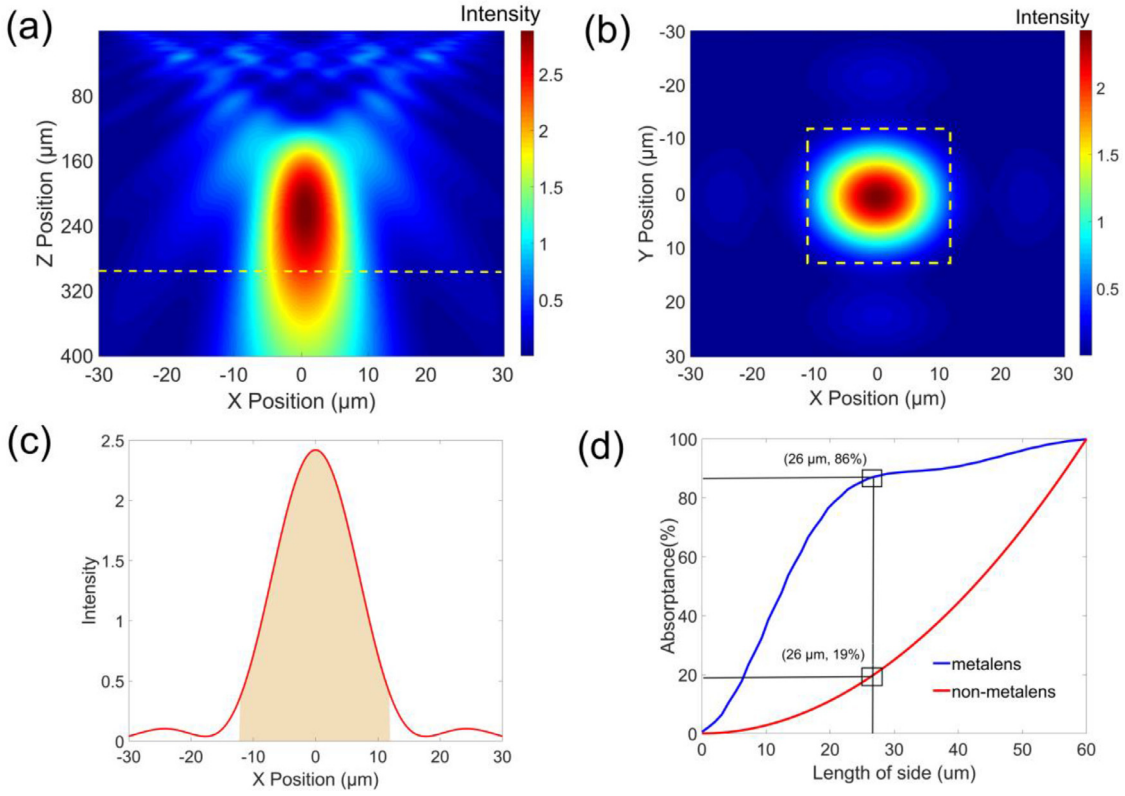

Fig. 3. Light field propagation simulation. (a) The light intensity distribution on the X-Z plane. (b) The light intensity distribution on the focal plane. (c) The cross-section of the intensity profile along the X-axis direction on the focal plane. (d) Absorptance of the photosensitive area of IR detector with or without metalens at various photosensitive areas.

Fig. 2(c) and (e) indicate that the subwavelength unit cells play the role of antireflective coating simultaneously. According to the Fresnel formula [23], the transmittance of the air-silicon interface can be calculated as 0.7. The effective refractive index of the metasurface layer is between air and silica dielectric, buffering the electromagnetic impedance mismatch. The average transmittance is increased to about 0.8, which improves the utilization efficiency of light energy. This antireflective characteristic is not possessed by spherical lenses and diffractive lenses with a period larger than the wavelength.

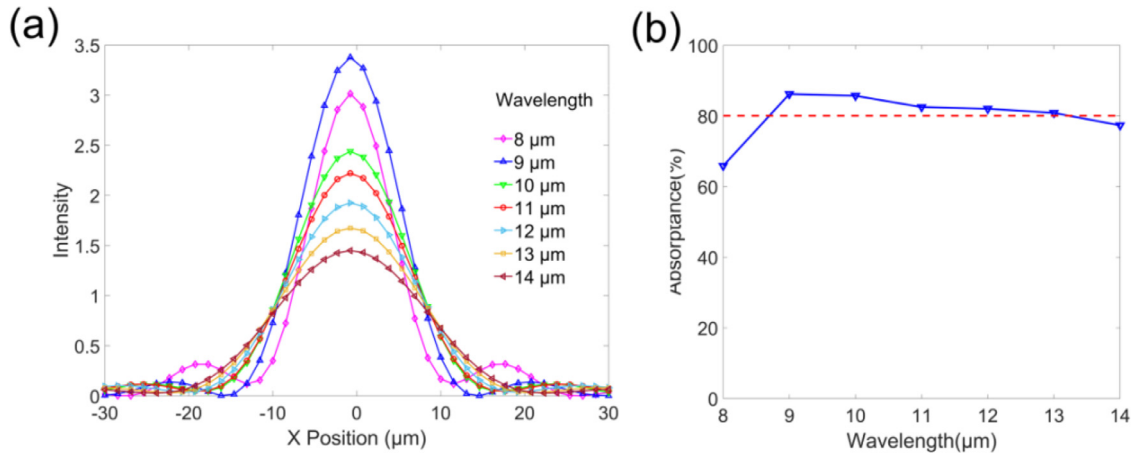

Fig. 4. The dispersion characteristic of the metalens. (a) The light intensity distribution for different wavelengths along the X-axis direction. (b) The absorptance of the IR detector for different wavelengths.

2.3. Light field propagation simulation

Infrared light field propagation was simulated for the metalens, and the results are shown in Fig. 3. The incident plane wave gradually converges after passing through the metasurface and is focused into a thin beam at the photosensitive region, and it is quickly absorbed after penetrating the IR absorber. The absorptance (here also referred to as the effective fill factor) is defined as the ratio of the energy in the photosensitive area to the total energy incident in the entire aperture. According to the calculation results (Fig. 3(d)), with the increase of the side length of the photosensitive area, the fill factor of the non-lens detector exhibits a concave quadratic increase. In contrast, the effective fill factor of the detector with the metalens increases rapidly. For a detector with a small photosensitive region, the improvement of absorptance becomes particularly significant after the detector is integrated with the metalens.

For a photosensitive area with a side length of 26 μm, the absorptance of detector integrated with metalens reaches 86% at the wavelength of 10 μm, while the absorptance of the detector without the metalens is only 19%, which means that the absorptance of the detector is quadrupled with the integration of the metalens. As a light concentrator of the infrared detector, the metalens needs to have the achromatic ability, maintaining a high focusing efficiency in a wide spectral range. Due to the structural dispersion characteristic, the chromatic aberration to the light field distribution is inevitable, as shown in Fig. 4(a). Nevertheless, with proper design, the absorptance within the spectrum of 8 μm to 14 μm can be controlled to be above 80% except for the slightly lower values at the edges of the spectrum as illustrated in Fig. 4(b). Therefore, the average absorptance in the entire LWIR reaches 80%, and the effective fill factor of the infrared focal plane array is significantly improved. For the imaging lens, the focal length changes with the incident wavelength due to chromatic aberration, which results in blurred images of the object. However, for the energy-concentrating lens, the effect of dispersion on the absorptance is limited. The lens does not require additional achromatic design, avoiding complicated structures that are difficult to manufacture.

3. Microfabrication process of the metalens

Considering the LWIR working range and the compatibility with the general MEMS process, the metalens consisting of silicon pillars is fabricated based on a silicon substrate. The detailed fabrication process is illustrated in Fig. 5. After the silicon substrate is cleaned, a 100 nm-thick aluminum film is deposited as a hard mask by electron beam evaporation (K.J. Lesker LAB 18). The big particles in the film evaporated by the electron beam will affect the accuracy during pattern transfer so that a high deposition rate is required to control particle size. Electron-beam lithography (EBL, JEOL, 6300FS) followed by inductively coupled plasma etch (Oxford, Plasma System100 ICP180) forms the hard mask on the aluminum film. The 8μm-thick structure layer of silicon is etched in a deep silicon etching system (Oxford, Estrelas 100) to ensure vertically etched sidewalls. Finally, the hard mask is removed by using the aluminum etchant, leaving the array of silicon pillars with various diameters.

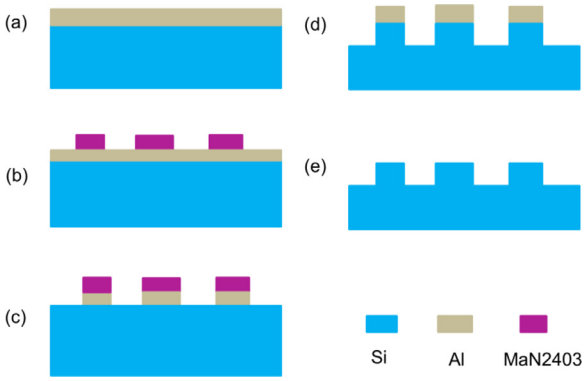

Fig. 5. Schematic showing the major steps of the fabrication process. (a) Deposition of the aluminum film by electron beam evaporation. (b) Patterning of MaN2403 using EBL. (c) Al hard mask etched by ICP. (d) Etching silicon to form the pillar array. (e) Removal of the hard mask.

The scanning electron microscopy (SEM, Hitachi, SU8220) images of the fabricated metalens are shown in Fig. 6 with a very small deviation from the designed geometric parameters of pillars. The individual pillar exhibits the vertical profile (Fig. 6(b)) and the smooth sidewall (Fig. 6(c)). The subwavelength silicon pillars can be regarded as waveguides constraining the optical field, and the small roughness on the sidewalls of the pillars will reduce the scattering losses of light during its propagation in the waveguides [24]. Some folds are found at the bottom of the pillars, which will bring errors to the phase modulation.

4. Investigation of focusing effect of the metalens

The experimental setup for measuring the focusing effect of the metalens is illustrated in Fig. 7(a). A hot plate with a temperature of 130 °C is used as the infrared radiation source. The patterned silicon sample with a 3 × 2 metalens array is mounted on a three-dimensional moving platform. An LWIR camera (FLUKE TiX660) with a microscope is

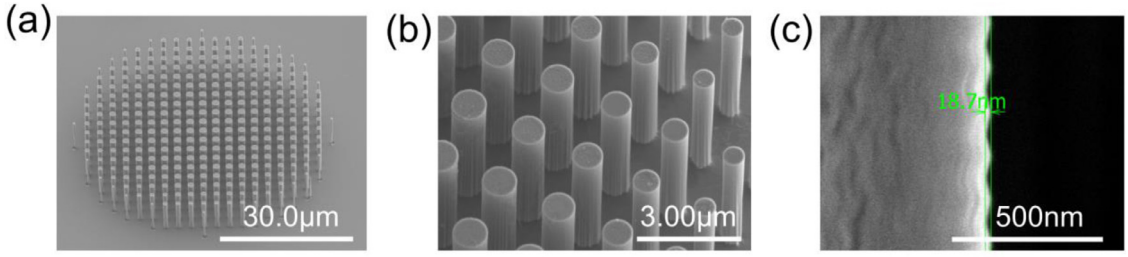

Fig. 6. (a) SEM image of the metalens with a diameter of 60 μm. (b) SEM image of individual pillars. (c) SEM image of the sidewall surface.

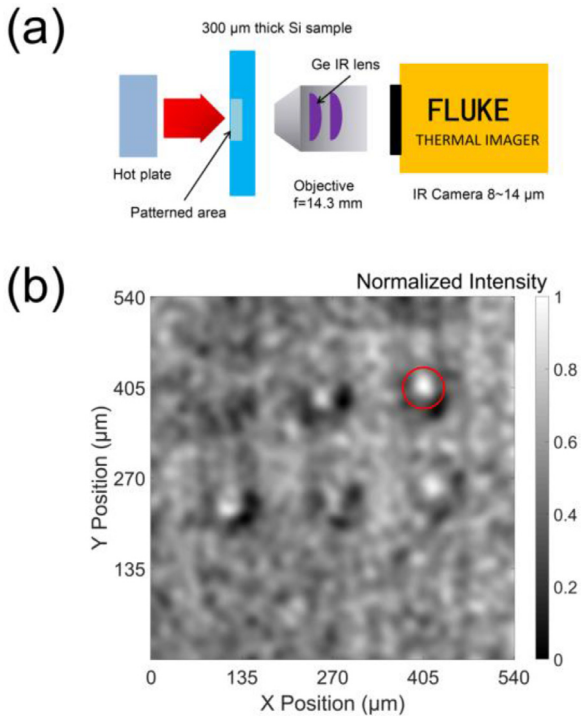

Fig. 7. (a) Experimental setup for measuring the focusing effect of the fabricated metalens. (b) Measurement results of the focusing effect.

used to observe the intensity distribution on the sample. The infrared irradiation from the hot plate can be approximated as parallel light considering the small aperture of the metalens and the sufficiently large distance (500 mm) between the hot plate and the metalens. Therefore, the infrared light irradiated on the metalens will converge into a spot at the back focal plane of the metalens. By adjusting the distance between the sample and the objective lens, bright spots with concentrated energy can be observed (Fig. 7(b)) when the object plane overlaps with the back focal plane of the metalenses. The aperture of the metalens is marked with a red circle. The size of the focal spot is smaller than the aperture, indicating that the metalens functions as a beam concentrator and can be used to increase the effective fill factor of the infrared detectors. Because the focal spot radius (13 μm) is close to the diffraction limit of the infrared microscope system, it is difficult to obtain precise intensity distribution. Considering the small manufacturing error demonstrated in Fig. 6, a slight deviation is expected between the actual focusing effect and the simulation.

5. Conclusion

In conclusion, we propose the design of monolithic integration of a long-wave infrared detector based on a silicon substrate and a metalens to improve the effective fill factor. The FDTD simulation shows that the metalens can concentrate 80% of the incident light energy within 20% of the pixel area, and the effective fill factor of the detector is quadrupled. The experimental measurement results show that the metalens can achieve a good focusing effect in the 8–14 μm region. The manufacturing process of the metalens is compatible with the architecture of the infrared detector, in which the metalens can be integrated into a large-scale focal plane array to improve the performance of the infrared thermal imager.

Furthermore, the ultra-high effective fill factor is achieved within 20% of the pixel area, which is much smaller than the absorption plate of many uncooled infrared detectors, especially optical readout uncooled infrared detectors [2–5]. Therefore, the length of the thermal insulation structure or the thermomechanical structure can be increased accordingly, leading to a smaller noise equivalent temperature difference (NETD) [4], which is of substantial significance for promoting the commercial use of optical readout uncooled infrared imaging.

Declaration of Competing Interest

The authors declared that they have no conflicts of interest to this work.

We declare that we do not have any commercial or associative interest that represents a conflict of interest in connection with the work submitted.

CRediT authorship contribution statement

Huwang Hou: Investigation, Software, Data curation, Visualization, Writing – original draft. **Yiyuan Zhang:** Writing – review & editing. **Zhendong Luo:** Investigation. **Peng Zhang:** Conceptualization, Methodology. **Yang Zhao:** Supervision, Project administration, Writing – review & editing.

Funding

This work was financed by the National Natural Science Foundation of China (#11772321 and #51732006).

Acknowledgments

We would like to thank the USTC Center for Micro and Nanoscale Research and Fabrication and Experimental Center of Engineering and Material Sciences of USTC for the support in the microfabrication process.

References

[1] Vollmer Michael, Möllmann Klaus-Peter. Infrared thermal imaging: fundamentals, research and applications. John Wiley & Sons; 2017.
[2] Toy MF, et al. Uncooled infrared thermo-mechanical detector array: design, fabrication and testing. Sensors Actuators A Phys 2009;156(1):88–94. doi:10.1016/j.sna.2009.02.010.
[3] Shang Y, et al. Design, fabrication, and characterization of a polymer-Based MEMS uncooled infrared focal plane array. J Microelectromech Syst 2015;24(4):1132–41. doi:10.1109/JMEMS.2014.2386871.

[4] Yang Z, et al. Optomechanical uncooled infrared imaging system: design, microfabrication, and performance. J Microelectromech Syst 2002;11(2):136–46. doi:10.1109/84.993448.
[5] Datskos PG, et al. Infrared imaging using arrays of SiO2micromechanical detectors. Opt Lett 2012;37(19):3966. doi:10.1364/OL.37.003966.
[6] Shang Y, et al. Coaxial dual-wavelength interferometric method for a thermal infrared focal-plane-array with integrated gratings. Sci Rep 2016;6:25993. doi:10.1038/srep25993.
[7] Li F, et al. HgCdTe mid-Infrared photo response enhanced by monolithically integrated meta-lenses. Sci Rep 2020;10(1). doi:10.1038/s41598-020-62433-w.
[8] Yan JH, et al. Design and fabrication of novel microlens–micromirrors array for infrared focal plane array. Microw Opt Technol Lett 2012;54(4):879–84. doi:10.1002/mop.26722.
[9] Allen KW, et al. Increasing sensitivity and angle-of-view of mid-waveinfrared detectors by integration with dielectric microspheres. Appl Phys Lett 2016;108(24):342–473. doi:10.1063/1.4954190.
[10] Du C, et al. Method for improving performance of IR focal plane array using microlens array. Proc of SPIE–Int Soc Opt Eng 1997;3099:107–14. doi:10.1117/12.281214.
[11] Bai J, et al. Performance optimization of InSb infrared focal-plane arrays with diffractive microlenses. J Electron Mater 2014;43(8):2795–801. doi:10.1007/s11664-014-3054-0.
[12] Yu Nanfang, et al. Light propagation with phase discontinuities: generalized laws of reflection and refraction. Science 2011;334(6054):333–7. doi:10.1126/science.1210713.
[13] Klopfer E, et al. Dynamic focusing with high-quality-factor metalenses. Nano Lett 2020;20(7):5127–32. doi:10.1021/acs.nanolett.0c01359.
[14] Khorasaninejad M, et al. Metalenses at visible wavelengths: diffraction-limited focusing and subwavelength resolution imaging. Science 2016;352(6290):1190–4. doi:10.1126/science.aaf6644.
[15] Rubin NA, et al. Matrix fourier optics enables a compact full-Stokes polarization camera. Science 2019;365(6448):eaax1839. doi:10.1126/science.aax1839.
[16] Yi F, et al. Plasmonically Enhanced Thermomechanical Detection of Infrared Radiation. Nano Lett 2013;13(4):1638–43. doi:10.1021/nl400087b.
[17] Yuan Y, et al. Terahertz dual-band polarization control and wavefront shaping over freestanding dielectric binary gratings with high efficiency. Opt Lasers Eng 2021;143(1):106636. doi:10.1016/j.optlaseng.2021.106636.
[18] Zhang S, et al. Solid-immersion metalenses for infrared focal plane arrays. Appl Phys Lett 2018;113(11) 111104.1-111104.5. doi:10.1063/1.5040395.
[19] Fan Q, et al. A high numerical aperture, polarization-insensitive metalens for long-wavelength infrared imaging. Appl Phys Lett 2018;113(20) 201104.1-201104.4. doi:10.1063/1.5050562.
[20] West PR, et al. All-dielectric subwavelength metasurface focusing lens. Opt Express 2014;22(21):26212. doi:10.1364/OE.22.026212.
[21] Chen X, et al. Longitudinal Multifoci Metalens for Circularly Polarized Light. Adv Opt Mater 2015;3(9):1201–6. doi:10.1002/adom.201500110.
[22] Wang S, et al. Wide-band achromatic flat focusing lens based on all-dielectric subwavelength metasurface. Opt Express 2017;25(6):7121. doi:10.1364/OE.25.007121.
[23] Born M. Principles of optics–Electromagnetic theory of propagation, interference and diffraction of light. DBLP; 1999. 7. ed..
[24] Yap KP, et al. Correlation of scattering loss, sidewall roughness and waveguide width in silicon-on-insulator (SOI) ridge waveguides. J Lightwave Technol 2009;27(18):3999–4008. doi:10.1109/JLT.2009.2021562.